# Spike Communication of Dynamic Stimuli: Rate Code versus Temporal Code*

David H. Goldberg and Andreas G. Andreou
Department of Electrical and Computer Engineering
Johns Hopkins University
3400 N. Charles St., 105 Barton Hall
Baltimore, MD 21218 USA

**Abstract**

We compare the efficacy with which two spike codes communicate information about a dynamic stimulus. We examine a rate code, which represents the stimulus by the number of spikes in a time window, and a temporal code, which represents the stimulus with interspike intervals. We model the distortion introduced by an integrate-and-fire encoder and two forms of noise—spike jitter and spike deletions. In the noiseless case, a temporal code based on single interspike intervals is superior to the rate code. In the presence of noise, the temporal code must average over several intervals in order to outperform the rate code.

## 1 Introduction

We compare the efficacy with which two spike codes communicate information about a dynamic stimulus. The first code is a rate code, in which the stimulus is represented by the number of spikes in a time window of length $T_w$. The second code is a temporal code, in which the stimulus is represented by the inverse of the time required for $K$ spikes. In the case of $K = 1$, the stimulus is represented by the inverse of the interspike interval (ISI), and this decoder is sometimes referred to as an interval code. We quantify the efficacy by comparing a continuous signal with a reconstruction of the signal derived from a decoded spike train. In addition to the distortion introduced by the encoding of the signal, we include two explicit sources of noise—spike jitter and spike deletions.

We acknowledge that efferent neurons probably do not attempt to reconstruct the somatic activity of afferent neurons. On the contrary, many rich forms of computation are implemented from one neuron to the next. However, because we are interested in isolating the properties of the spike codes themselves, we believe this reconstruction paradigm is appropriate, as it provides an upper limit on the amount of information that is available for neuronal computation.

The performance of rate codes and temporal codes have been compared qualitatively [2, 5] and quantitatively [3, 1, 4]. In these works, the authors looked at the information capacity of

*Thanks to Arun Sripati, Pamela Abshire, Harel Shouval, and Brian Blais for helpful discussions.

the spike coding schemes. While the information capacity elucidates the limitations of the spike codes themselves, its use assumes that the encoding of the signal is lossless. In this work, we consider realistic band-limited signals and how encoding them in the form of spike trains degrades information transfer. Therefore, we consider the distortion as an alternative to the information capacity.

# 2 Methods

We have developed a simple mathematical framework to analyze the performance of spike codes (Fig. 1). This framework captures many elements of real neurons, yet is simple enough to provide analytical results. We quantify the performance of the coding schemes by the determining the distortion incurred by spike coding—lower distortion corresponds to higher performance. The distortion is given by a mean squared error between the stimulus $W$ and the reconstruction $\hat{W}$:

$$\varepsilon^2 = E[(W - \hat{W})^2] \tag{1}$$

For both of the codes we analyze, the encoding and noise processes are identical—the only thing that differs is the decoding process.

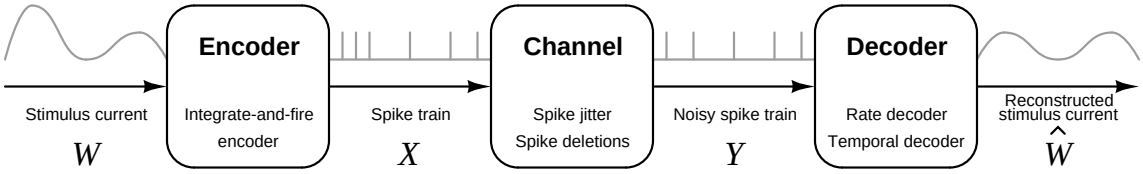


Figure 1: Framework used to assess the performance of the spike coding schemes.

**Input** To model the subthreshold activity in the soma, we use a stimulus current $W$ that has a Gaussian amplitude distribution (mean $\mu_W$ and variance $\sigma_W^2$) and a low-pass frequency characteristic. The power spectral density and autocorrelation of $W$ are given by

$$S_{WW}(\omega) = \frac{2\omega_c\sigma_W^2}{\omega_c^2 + \omega^2} + 2\pi\mu_W^2\delta(\omega) \leftrightarrow R_{WW}(\tau) = \sigma_W^2 e^{-\omega_c|\tau|} + \mu_W^2 \tag{2}$$

where $\omega_c$ is the cut-off frequency (rad/sec).

**Spike encoding** Spike encoding in the axon hillock is represented by an integrate-and-fire encoder which converts the input current into a spike train $X$. The current charges a capacitance $C$, and when the voltage on the capacitor $V$ reaches the threshold $\theta$, a spike is emitted and $V$ is reset to zero. We can express the spike train $X$ in terms of its ISIs $\{T_i^X\}$ and spike times $\{t_i^X\}$ as recursive function of $W$:

$$\theta = \frac{1}{C}\int_{t_{i-1}^X}^{t_{i-1}^X + T_i^X} W(t)dt \tag{3}$$

The spike train can be expressed as the sum of shifted delta functions:

$$x(t) = \sum_i \delta(t - t_i^X) \tag{4}$$

The mean ISI $\mu_T$ and the mean spike rate $\lambda$ can be expressed in terms of the integrate-and-fire parameters as follows:

$$\mu_T = \frac{1}{\lambda} = \frac{C\theta}{\mu_W} \tag{5}$$

**Channel** Axonal communication and synaptic transmission are represented by a channel that corrupts the spike train $X$ by jittering and randomly deleting spikes, giving a noisy spike train $Y$. We model the spike jitter as a Gaussian random process that distorts the ISIs. Let $N$ be a Gaussian random variable where $N_i \sim \mathcal{N}(0, \sigma_{\text{ISI}}^2)$. Then $Y$ is given by

$$T_i^Y = T_i^X + N_i \tag{6}$$

We model spike deletions by modulating the spike train with a Bernoulli process. Let $B$ be a Bernoulli random variable where $P(B_i = 1) = p$ and $P(B_i = 0) = 1 - p = q$. Then $Y$ is given by

$$y(t) = \sum_i B_i \delta(t - t_i^X) \tag{7}$$

**Spike decoding** The postsynaptic transformations at the efferent neuron are represented by the spike decoding process, which gives a reconstruction of the stimulus current ($\hat{W}$). For the rate decoder, the reconstruction is given by

$$\hat{W}(t) = C\theta \left( \frac{n(t)}{T_w} \right) \tag{8}$$

where $n(t)$ is the number of spikes in a sliding counting window given by $[t - T_w, t]$. For the temporal decoder, the reconstruction is proportional to the time required for $K$ spikes:

$$\hat{W}(t) = C\theta \left( \frac{K}{\sum_{j=K-1}^{0} T_{i-j}} \right), \quad t_{i-K+1} < t < t_{i+1} \tag{9}$$

For $K = 1$, the reconstruction is proportional to the inverse of the current ISI, and the decoder is referred to as the interval decoder. In this formulation, $T_w$ and $K$ are free parameters that can be adapted to give optimal performance in a given situation. In all cases, the decoders are formulated such they are unbiased estimators of the input, and the reconstructions are properly aligned in time with the input.

# 3 Distortion models

In this section, we give expressions for the distortion of the rate code and the temporal code, and we show how spike jitter and spike deletions contribute to the distortion. Because all of the noise sources we consider are independent, the distortion expressions can be summed to give the total distortion. All models have been validated with simulations (not shown).

## 3.1 Rate code

**Low-pass noise** A significant component of the distortion arises as a result of the intrinsic low-pass filtering of the integrate-and-fire encoder. This can be modeled by the convolution of the input signal $W(t)$ with a rectangular window $h(t)$. The distortion is given by

$$\varepsilon^2_{\text{lowpass}} = \sigma^2_W - 2\text{Cov}(W,\hat{W}) + \sigma^2_{\hat{W}} \tag{10}$$

where

$$K_{W\hat{W}}(\tau) = K_{WW}(\tau) * h(\tau) \qquad \text{Cov}(W,\hat{W}) = K_{W\hat{W}}(0) \tag{11}$$

$$K_{\hat{W}\hat{W}}(\tau) = h(\tau) * K_{W\hat{W}}(\tau) \qquad \sigma^2_{\hat{W}} = K_{\hat{W}\hat{W}}(0) \tag{12}$$

**Quantization noise** The rate decoder has an additional intrinsic noise source which arises from the discrete nature of spike counts, which we term quantization noise. The quantization step is given by setting $n(t) = 1$ in Eq. 8:

$$\Delta = \frac{C\theta}{T_w} \tag{13}$$

It can be shown that the distortion arising from quantization noise is

$$\varepsilon^2_{\text{quant}} = \Delta^2/6 \tag{14}$$

**Spike jitter** The effect of spike jitter on the rate code is subtle. Jitter causes a spike to be pushed into or out of a counting window. The distortion due to this effect, $\varepsilon^2_{\text{jitter}}$, can be found by taking into account the Gaussian distribution of the spike jitter (expression not shown).

**Spike deletions** The number of spikes in a window that are preserved following deletion is given by the binomial distribution. The distortion due to spike deletion is given by

$$\varepsilon^2_{\text{deletion}} = \left(\frac{T_w}{\mu_T}\right)\left(\frac{q}{p}\right)\Delta^2 \tag{15}$$

## 3.2 Temporal code

**Low-pass noise** The temporal code is also subject to the low-pass effects of the integrate-and-fire encoder, and the expression given by the Eq. 10 is valid. However, the expressions for the covariance $K_{W\hat{W}}(0)$ and variance $\sigma^2_{\hat{W}}$ are not given as simply as Eqs. 11 and 12, but analytical solutions have been found (not shown).

**Spike jitter** Spike jitter corrupts the ISIs, so its effect on the interval decoder is straightforward. The distortion can be found by a propagation of error approach:

$$\varepsilon^2_{\text{jitter}} = \frac{\mu^2_{\hat{W}}\sigma^2_{\text{ISI}}}{(K\mu_T)^2} \tag{16}$$

**Spike deletion** The deletion of spikes introduces distortion for the temporal decoder. For example, the deletion of a single spike causes the two intervals delimited by the spike to be merged into a single interval, the length of which is given by the sum of the two original intervals. The general expression is given by

$$\varepsilon^2_{\text{deletion}} = \sum_{y=0}^{\infty}\sum_{x=0}^{\infty} x\left[\mu_W\left(1-\frac{K}{p(x+y)}\right)\right]^2 pP_X(x)P_Y(y) \tag{17}$$

where $P_X(x)$ is the geometric density function and $P_Y(y)$ is the negative binomial density function with $r = K-1$.

# 4 Results

In this section, we compare the rate code and the temporal code and determine how the noise level influences the performance of the codes. The models enable us to freely explore the parameter space without having to resort to extensive simulations. For the rate code, the length of the spike counting window $T_w$ is a free parameter. For the temporal code, the number of ISIs considered $K$ is a free parameter. The $K$ parameter can be converted to an effective window size by multiplying by the mean ISI $\mu_T$ for comparison with $T_w$.

**Noiseless case** In the noiseless case, the temporal code is superior to rate code at all window sizes (Fig. 2(a)). The optimal temporal code is the interval code ($K = 1$). The optimal rate code occurs at the window that optimizes the trade-off between low-pass noise and quantization noise. For long windows, the performance of the temporal code approaches that of the rate code, as the information contained individual ISIs is averaged away, and the rate code's quantization noise diminishes.

**The effect of noise** In the presence of noise in the form of spike jitter (Fig. 2(b)) or spike deletions (Fig. 2(c)), the temporal code still remains superior to the rate code. However, the temporal code must average over several intervals to obtain optimal performance. The rate code is very robust to spike jitter, but spike deletions shift the optimal window size to higher values.

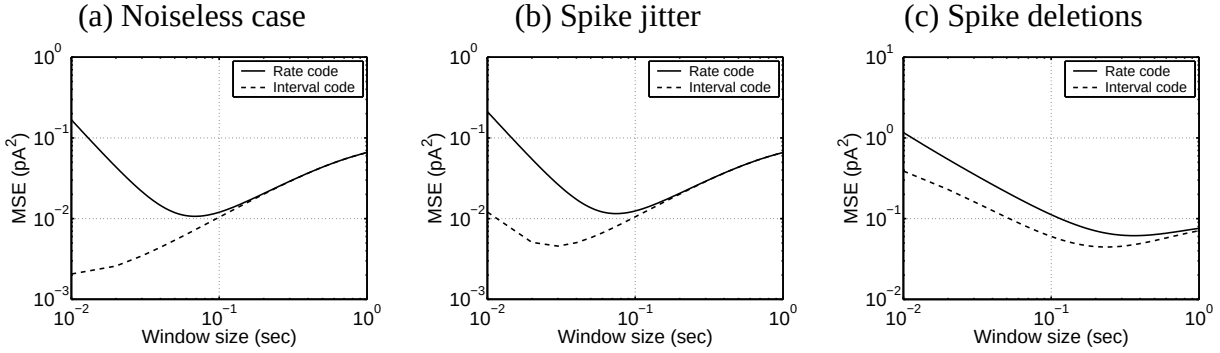


Figure 2: Comparison of the rate code and the temporal code (parameters given in Appendix A). (a) Noiseless case. (b) Spike jitter, $\sigma_{\text{ISI}} = 10^{-3}$ sec. (c) Spike deletions, $q = 0.5$.

# 5 Future work

The work presented here elucidates the intrinsic limitations of the spike coding schemes and demonstrates how these schemes are influenced by physiological noise sources. This is part of our larger goal—to be able to make predictions about the nature of a spike coding for a given system on the basis of measurable physiological parameters.

The focus of future work is recast these decoders in terms of physiologically plausible mechanisms such as linear filtering of the spike train for rate decoding, and non-linear filtering of the spike train by means of short-term synaptic dynamics for temporal decoding. We are also exploring the effects of transmitting information with parallel channels. We find that using multiple encoders with different initial conditions enables better performance because the encoders can capture multiple phases of the signal. For the rate code, parallel channels permits the use very small windows, transforming the rate code into a space code.

# A Nominal parameters

The parameters used to generate Fig. 2 are given below:

| Symbol | Description | Value | Units |
|---|---|---|---|
| $\mu_W$ | Mean input current | 1 | $\mu$A |
| $\sigma_W^2$ | Input current variance | 0.1 | pA$^2$ |
| $\omega_c$ | Input current bandwidth | $2\pi$ | rad/sec |
| $\lambda$ | Mean spike rate | 100 | Hz |
| $\mu_T$ | Mean ISI | $1/\lambda$ | sec |
| $C$ | Membrane capacitance | 1 | $\mu$F |
| $\theta$ | Spike threshold | $\mu_I/(\lambda C)$ | V |
| $\sigma_{\text{ISI}}$ | ISI jitter | $10^{-3}$ | sec |
| $p$ | Spike preservation probability | 0.5 | — |
| $q$ | Spike deletion probability | $1-p$ | — |

# References


[1] R. Eckhorn, O. J. Grüsser, J. Kröller, K. Pellnitz, and B. Pöpel. Efficiency of different neuronal codes: Information transfer calculations for three different neuronal systems. *Biological Cybernetics*, 20:49–60, 1976.

[2] Donald M. MacKay and Warren S. McCulloch. The limiting information capacity of a neuronal link. *Bulletin of Mathematical Biophysics*, 14:127–135, 1952.

[3] Anatol Rapoport and William J. Horvath. The theoretical channel capacity of a single neuron as determined by various coding schemes. *Information and Control*, 3:335–350, 1960.

[4] William R. Softky. Fine analog coding minimizes information transmission. *Neural Networks*, 9:15–24, 1996.

[5] Richard B. Stein. The information capacity of nerve cells using a frequency code. *Biophysical Journal*, 7:797–826, 1967.